ELSEVIER

Thin Solid Films 345 (1999) 244–254

thin solid films

Spin-on-glass thin films prepared from a novel polysilsesquioxane by thermal and ultraviolet-irradiation methods

Qi Pan[a], Gabriela B. Gonzalez[a], Russell J. Composto[a,*], William E. Wallace[b], Barry Arkles[c], Lisa K. Figge[d], Donald H. Berry[d]

[a]*Laboratory for Research on the Structure of Matter and Department of Materials Science and Engineering, University of Pennsylvania, Philadelphia, PA 19104, USA*

[b]*Polymers Division, National Institute of Standards and Technology, Gaithersburg, MD 20899, USA*

[c]*Gelest, Inc., Tullytown, PA 19007, USA*

[d]*Laboratory for Research on the Structure of Matter, and Department of Chemistry, University of Pennsylvania, Philadelphia, PA 19104, USA*

Received 8 July 1998; received in revised form 21 November 1998; accepted 22 November 1998

Abstract

New dielectric films are prepared by both pyrolytic and photolytic conversion of β-chloroethyl-silsesquioxane (BCESSQ). Film thickness, refractive index, composition, density and morphology are characterized using a palette of techniques including ellipsometry, Rutherford backscattering and forward recoil spectrometry, X-ray reflectivity, and atomic force and electron microscopies. After annealing at 350°C, BCESSQ films, initially 200 nm thick reach about 55% of their original thickness after 20 min. For films heated in air for 4 h, the atom fractions of carbon and hydrogen monotonically decrease to 10 and 30%, respectively, as annealing temperature increases from 225 to 450°C. The BCESSQ reactivity is reflected in the loss of chlorine at 400°C. At 450°C, the film density is 1.88 g/cm^3, or 84% of thermally-grown silicon oxide. Upon exposure to ultraviolet ozone radiation, films ranging from ca. 200 to 700 nm are found to convert to ormosil films within 30 min. Surprisingly, the chlorine concentration is found to decrease more quickly than the hydrogen and carbon concentrations, suggesting that the ormosil film evolves HCl leaving a vinyl group of $Si{-}CH{=}CH_2$. This reaction pathway differs from the thermal case. For films prepared by pyrolytic and photolytic methods, atomic force and electron microscopy studies show that the surface is smooth and featureless, the bulk is void free when view at a magnification of 50 000 ×, and the ormosil/substrate interface is continuous. © 1999 Elsevier Science S.A. All rights reserved.

Keywords: Dielectrics; Polymers; Rutherford backscattering spectroscopy; Silicon oxide

1. Introduction

Dielectric materials for ultralarge scale integration (ULSI) interlayer applications have been extensively reviewed [1]. As recently pointed out, future improvements in integrated circuit technology will require the development of new dielectric materials [2,3]. From this prospective, the 'materials' challenge is to satisfy the electrical, chemical, mechanical and thermal demands placed on the next generation of dielectric materials. Property requirements include low dielectric constant, high breakdown voltage, good mechanical strength, high thermal stability during processing, etch selectivity, chemical resistance, good adhesion, low stress, and superior gap-fill and planization properties [2]. Dielectric films are mainly prepared by vapor deposition or spin-on coating techniques. The vapor deposition is attractive because it is solventless, covers large areas with 2% uniformity in relative thickness, has excellent gap-filling capabilities, and operates at low temperatures [4]. Vapor deposition can also be used to deposit insoluble fluorinated polymers, like polytetrafluoroethylene, with extremely low dielectric constants (e.g. 1.8–3.0). Unfortunately, most fluoropolymer films lack the adhesive and plastic creep properties required for microelectronic applications [4].

In this paper, we focus on silicon oxide materials prepared by the facile spin casting technique for interlayer dielectric applications. Typically, silicon oxide films are prepared by heating silicon in oxygen or steam at high temperatures, ca. 1000°C. Because of their quality and extensive history, the properties of thermal silicon oxide films are an important benchmark for new dielectric materials. Selected characteristics include a dielectric constant of

* Corresponding author.
E-mail address: composto@lrsm.upenn.edu (R.J. Composto)

0040-6090/99/$ - see front matter © 1999 Elsevier Science S.A. All rights reserved.
PII: S0040-6090(98)01740-4

≈ 4, a refractive index of 1.462@546 nm, a *P*-etch rate of 2.0 Å/s, and a density of 2.2 g/cm^3 [5]. Because of their high processing temperature, silicon oxide films produce a large thermal stress in multilevel integrated circuits, which can lead to device failure. Thus, low-temperature routes for preparing silicon oxide films are very attractive. For example, a plasma-enhanced chemical vapor deposition technique has produced fluorine doped silicon oxides with a low dielectric constant, 3.1 [6]. Unfortunately, only a limited fluorine content can be incorporated before hydrolysis of Si—F bonds leads to an unstable film. Similar to the fluorinated polymers, these films also show poor adhesive properties. Silicon oxide films can also be prepared from a monomer like tetraethoxysilane, (TEOS) $[Si(OC_2H_5)_4]$or a polymer like poly(dimethylsiloxane) (PDMS)$[SiO(CH_3)_2]$. In either case, the starting material can be transformed to silicon oxide by heating in air or oxygen, rapid thermal annealing, or exposure to ultraviolet-ozone radiation. In addition to driving the chemical reaction to completion, the transformation conditions aim to remove reaction products like hydrocarbons and provide material transport to seal voids (i.e. raise film density). For example, PDMS films can be converted to silicon oxide films by heating at 800°C or higher [7]. Unfortunately, thick, crack-free films are difficult to prepare from siloxane films. Typically, thicknesses are limited to about 400 nm [31]. Furthermore, the high processing temperature is not a significant improvement over the thermal oxide route.

Silsesquioxanes (SSQ) are attractive materials for microelectronic applications such as interlayer dielectrics [8]. Hydrogensilsesquioxanes (HSSQ) are thought to be branched linear molecules with Si—O backbones where each silicon is attached to two backbone oxygens, one bridging oxygen, and one hydrogen to form a ladder structure. Polyhedral cage structures of HSSQ ($Si_8O_{12}H_8$) are particularly attractive because they convert to silica at relatively low processing temperatures, 350–400°C [9]. One strategy for reducing the dielectric constant is to incorporate carbon into oxide films. For example, the dielectric constant of methylsilsesquioxanes (MSSQ) is 2.7, whereas it is 2.9 for HSSQ [9]. Because of the Si—C bond, phenylsilsesquioxane (PSSQ) is extremely stable and does not begin to lose mass until 525°C in air [8].

In this paper we aim to follow the conversion of a new polymer precursor, namely β-chloroethyl-silsesquioxane (BSCESSQ), to a silicon oxide film deposited on a silicon substrate. As shown by compositional analysis, these oxide films are more accurately called ormosils, for organically-modified silica [10], because they form molecular composites of inorganic and organic materials. The BCESSQ molecules form both ladder and cage structures, where the substituent on the silicon atom is a BCE group. In contrast to the other SSQ's, the thermal transformation of BCESSQ occurs by a two stage hydrolysis route [11]. Initially, thermal cleavage of BCE results in the elimination of ethylene and the migration of the β-chlorine to silicon. Although the mass loss occurs predominantly during this stage, the material is a viscoelastic polymer of moderate molecular mass. Therefore, by-products are easily removed and subsequent voids are filled. During the second stage, a condensation reaction leads to the elimination of hydrogen chloride and a rigid ormosil film. A main advantage of the BCESSQ chemistry is the controlled release of reaction products and the retarded formation of rigid quaternary oxygen-bonded silicon atoms. Compared to the other SSQ's, a more dense film is expected. Moreover, by limiting the extent of reaction, the carbon content can be tuned to produce a film with a wide range of dielectric properties.

Using pyrolytic and photolytic methods to prepare ormosil films, the film thickness, refractive index, composition and density are determined. Although stable at room temperature, BCESSQ films partially convert to ormosil films at temperatures as low as 225°C. Upon increasing the processing temperature from 225 to 450°C for 4 h in air, the carbon and hydrogen concentrations monotonically decrease to 10 and 30 at.%, respectively. The high reactivity of the BCE group is reflected in the complete removal of chlorine at 400°C. At 450°C, the film density is 1.88 g/cm^3, or 84% of a thermal silicon oxide. BCESSQ films ranging from ca. 200 to 700 nm are found to convert to ormosil films very rapidly (i.e. within 30 min) upon exposure to ultraviolet radiation. Conversion is observed to occur uniformly through the film. Surprisingly, the chlorine concentration is found to decrease more quickly than the hydrogen and carbon concentrations, suggesting that the ormosil film evolves HCl initially leaving a vinyl group of Si—CH=CH_2. This reaction pathway differs from the thermal case described above. For films prepared by pyrolytic and photolytic methods, atomic force and electron microscopy studies show that the surface is smooth and featureless, the bulk is void free at 50 000×, and the ormosil/substrate interface is continuous.

2. Experimental procedures

2.1. Materials

The synthesis of β-chloroethyl-silsesquioxane (BCESSQ) has been presented [11]. The silicon atoms are linked by oxygen bridges and attached to pendant β-chloroethyl groups. The linear molecules form a ladder structure whereas the cage-like molecules form dimers, trimers and small oligmers. Subsequent polymerization occurs after (5–7) days to produce the polymer used in this study. The mass average relative molecular mass and the number average relative molecular mass are 10 400 and 4600 u, respectively, as measured by gel permeation chromatography using polystyrene standards. Using IR and NMR to determine the silanol, Si—OH, concentration, the BCESSQ composition is nominally $[(ClC_2H_4)SiO_{1.5}]2[(ClC_2H_4)$-$Si(O)OH]$.

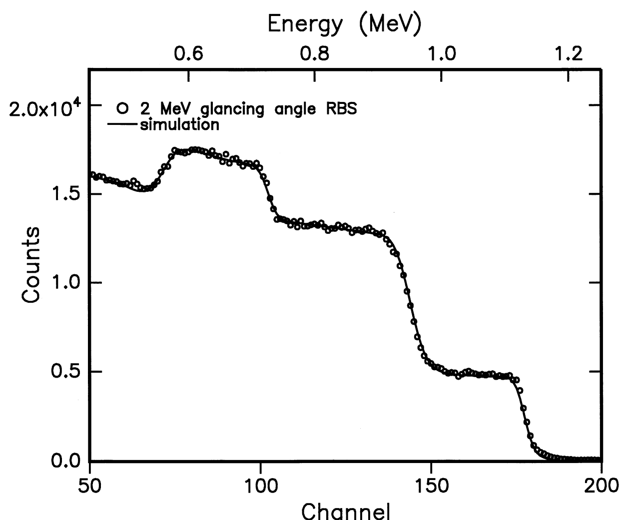

Fig. 1. Rutherford backscattering spectrometry spectrum for 2.0 MeV He^+ ions incident on a silicon substrate covered with a 100 nm ormosil film prepared from BCESSQ at 400°C for 4 h. The surface energies for silicon and oxygen in the film are located near 1.13 and 0.72 MeV, respectively. The solid line is a simulation based on the composition in Table 1.

As a reference, thin film characterization is also carried out on commercial, low dielectric constant materials donated by Allied Signal1. The Accuspin® 720, a spin-on polymer, is supplied as a solution of polysiloxane and n-propoxypropanol. Following the manufacturer's guidelines, the Accuspin film was heated in a nitrogen atmosphere from 20 to 275°C in about 10 min and then ramped from 275 to 400°C in 4 min. After conversion, the Accuspin film is pink in color with an ellipsometric thickness of 297.0 nm Accuglass® 3111, a spin-on glass, is supplied as a solution of poly(methylsiloxane) dissolved in ethyl alcohol, isopropanol, acetone, and n-butyl alcohol. The Accuglass1 film was heated for 1 min at 100, 150 and 250°C and cured at 425°C for 1 h in nitrogen. This film was pink with a thickness of 273.0 nm.

2.2. Bulk thermal analysis

In this section, the bulk characterization of BCESSQ will be summarized [11,12]. Thermogravimetric analysis (TGA) at a heating rate of 10°C /min in air showed that BCESSQ mass loss begins slowly at 150°C, and then more rapidly between 200 and 400°C. Simultaneous TGA-mass spectrometry analysis showed evidence of 26 and 35 u species starting at about 150 and 200°C, respectively. As discussed in [11], the initial reaction involves the elimination of ethylene with the migration of the β-chlorine to the silicon. Subsequently, a hydrolysis reaction produces hydrogen chloride leaving a cross-linked structure. At 450°C, the rapid mass loss stopped leaving about 55% of the initial mass. This value is very close to the calculated mass loss of 52.5% for the complete conversion of BCE to silica.

In isothermal TGA experiments at 300°C, the BCESSQ mass decreased monotonically with time until reaching 62% of the initial mass after 4 h. At 400°C, the mass reached a lower value, 55%, after only 1 h.

2.3. Thin film preparation

Thin BCESSQ films were spin coated from a diglyme solution onto silicon (100) wafers. The silicon wafers were first placed in a UV-ozone cleaner for 10 min to remove organic contaminants. Then the silicon was placed in a buffered oxide etch solution for 1 min to remove the native silicon oxide layer. The silicon was then rinsed with distilled water and dried under nitrogen flow until spin coating.

BCESSQ films were spin coated at a spin speed of 2000 r/min for 60 s. To partly remove solvent, these films were placed in a vacuum dessicator overnight. As-cast films with ellipsometric thicknesses of 200 to 700 nm, respectively, were prepared. These thicknesses agree with values determined by profilometry.

The ultraviolet induced transformation of BCESSQ films was performed with a Jelight Model 42 UVO-Cleaner®. (Certain commercial products are named to specify adequately the experimental procedure. This in no way implies endorsement nor recommendation by NIST.) The radiation is produced by a high-intensity low-pressure mercury vapor grid lamp, which produces intense UV radiation at 184.9, 253.7, and 282.1 nm. Exposure time was varied from 10 to 90 min.

2.4. Thin film characterization

Rutherford backscattering spectrometry (RBS) and forward recoil spectrometry (FRES) were used to determine

Table 1
Effect of temperature on thin film composition after 4 h in air

Temperature (°C)	Atom fraction (% Si)	Atom fraction (% O)	O:Si ratio	Atom fraction (% C)	Atom fraction (% Cl)	Atom fraction (% H)
As-cast[a]	10.0	16.7	1.7	20.0	10.0	43
225	9.0	16.0	1.8	17.0	5.0	55
300	14.0	26.0	1.9	17.0	1.0	42
400	17.0	36.0	2.1	14.0		38
450	18.0	42.0	2.3	10.0	—[b]	30

[a] Calculated from $[(BCE)SiO_{1.5}]_2[(BCE)Si(O)OH]$ [12].
[b] Below detection limits.

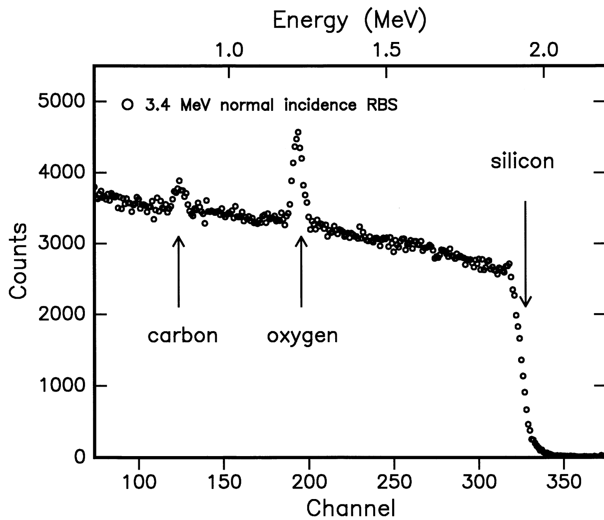

Fig. 2. Rutherford backscattering spectrometry spectrum for 3.4 MeV He^+ ions incident on the same sample as in Fig. 1. Due to the enhanced carbon cross-section, the carbon yield is clearly observed in contrast to the 2.0 MeV He^+ case in Fig. 1.

the heavy (i.e. Si, O, C and Cl) and light (i.e. H) atomic concentrations. The details of RBS [18,30] and FRES [16] have been presented. Fig. 1 shows the 2.0 MeV $^4He^+$ RBS spectrum from a BCESSQ film (ca. 100 nm thick) annealed at 400°C for 4 h deposited on silicon. To increase the path length of $^4He^+$ in the film, the sample is tilted 75° with respect to normal. The backscattering angle is 165° and the angle between the incident and backscattered ions is 15°. In Fig. 1, the surface yields for silicon and oxygen in the film are located near 1.13 MeV and 0.72 MeV, respectively. The back-edge yield for oxygen is found near 0.56 MeV. The oxygen energy width is used to determine the film areal density, Nt, where N and t are the atomic concentration and thickness, respectively. Note that the oxygen yield sits on top of the silicon substrate background, which starts near 0.95 MeV. From the measured yields, the oxygen and silicon atomic concentrations are calculated using the known cross-sections [18,30]. The solid line in Fig. 1 corresponds to a RUMP® simulation [13,14] using the composition found in Table 1. Note that the Cl signal is not detected. In Fig. 1, the carbon signal is also not observed both because of its low concentration and small scattering cross-section.

One objective of this study is to monitor the BCESSQ thin film composition, including C and H, as a function of processing conditions (e.g. temperature, time, UV exposure). In contrast to 2.0 MeV RBS, 3.4 MeV $^4He^+$ RBS was found to be highly sensitive to C because the cross-section is enhanced by a factor of six relative to the Rutherford cross-section [15]. Fig. 2 shows the 3.4 MeV $^4He^+$ spectrum from the same BCESSQ film as in Fig. 1. The geometry is the same as before except for the sample tilt, 7°. Note that the oxygen and carbon signals are clearly observed near 1.25 and 0.8 MeV, respectively. Both oxygen and carbon signals are superimposed on a large silicon background signal. The silicon yield from the film is buried by the silicon substrate signal. The hydrogen concentrations were determined by FRES [16]. In FRES, the incoming $^4He^+$ recoil the lighter H nuclei from the film. The recoiled H nuclei enter a solid-state detector which is located 30° from the incident beam direction and covered by a 7.5 μm Mylar stopper foil. Fig. 3 shows a 2.0 MeV $^4He^+$ FRES spectrum taken from the same film analyzed by RBS (cf. Figs. 1 and 2). The H concentration is directly proportional to the peak area. The solid line is a RUMP® simulation based on the composition in Table 1.

For RBS analysis of a sample containing light atoms in a heavy atom matrix, the sensitivity depends on the counting statistics associated with the heavy atom background under the light atom signal and errors associated with background subtraction [17]. For example, the O signal in Fig. 1 is superimposed on the silicon background. For Rutherford scattering from C, O and Cl in SiO_2, the detection limits expressed as atom fractions are 1.0, 0.5, and 0.2%, respectively [18]. Note that these limits do not include the background subtraction error. As shown in Fig. 3, the FRES spectrum only includes the hydrogen signal. For 20 μC of integrated charge and 10% estimated standard uncertainty, the total sensitivity for hydrogen in SiO_2 is around 2.0% expressed as an atom fraction.

The elemental uncertainties were determined by taking spectra of the same sample at 0°, 7° and 20°. For Si, O, Cl and H the estimated relative standard uncertainty was between ± 0.04 and ± 0.08 times the reported percentage. For C the estimated relative standard uncertainty was somewhat higher at ± 0.1 times the reported percentage. To a large extent, the composition uncertainty was due to ion beam damage during analysis. This damage was reduced by the methods below.

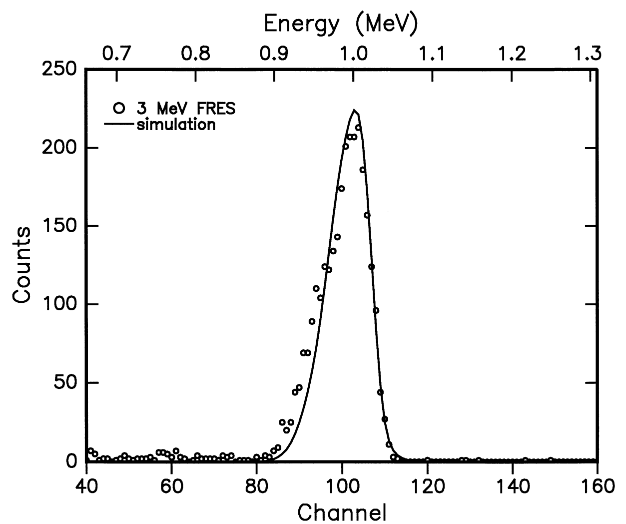

Fig. 3. Forward-recoil scattering spectrum for 2.0 MeV He^+ ions incident on the same sample as in Fig. 1. This spectrum provides the absolute hydrogen concentration.

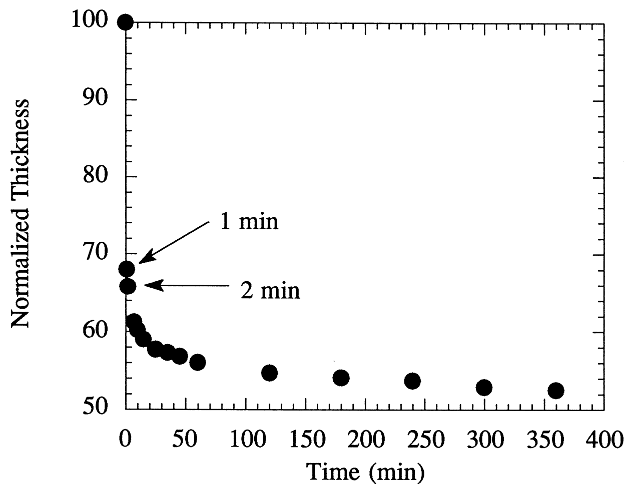

Fig. 4. Normalized film thickness (final thickness/initial thickness) as a function of annealing time at 350°C. The initial thickness is 206.5 nm.

The as-cast and partially converted films (i.e. low-temperature or short exposure times) were ion beam sensitive. These films underwent further conversion during ion beam analysis. The C, Cl and H signals were influenced by incident dose. Because ion dose is just another form of radiation, this influence is not surprising but rather provides an interesting potential means for controlling the depth distribution of the conversion. Neither the Si or O signals were found to depend on dose. For the annealing studies, RBS and FRES spectra were acquired at integrated charges of (1, 2, 3, 4, 5, 7, 10) μC. Subtracting the silicon background, the logarithm of the integrated areas for each element was plotted against the integrated charge. By extrapolation to zero charge, the correct counts was found for each element and, subsequently, used to determine the film stoichiometery. Using this procedure required 21 spectra per sample. To shorten analysis time, damage to the UV exposed films was reduced by moving the beam to a fresh spot on a 4 × 4 cm sample after each 1 μC dose. Ten spectra were then added to provide a 10 μC dose. This method greatly reduced data collection time.

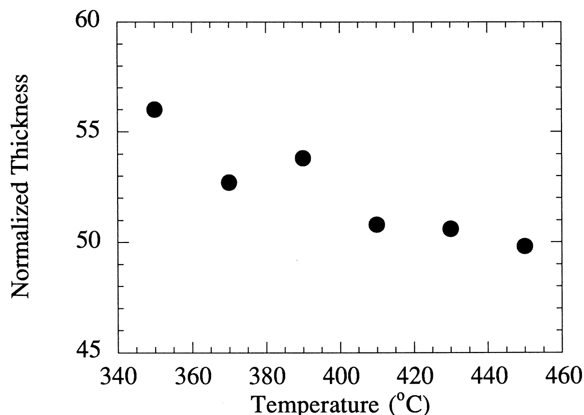

Fig. 5. Normalized film thickness as a function of annealing temperature for films annealed for 2 h at various temperatures.

X-ray reflectivity, XR, is a powerful method for measuring thin film density. In XR, one measures the grazing-incidence critical angle, a very sensitive measure of the film electron density. One disadvantage of single wavelength XR is that sample alignment can lead to uncertainty in measuring the critical angle. Energy dispersive XR eliminates some of this uncertainty by measuring the critical angle at many wavelengths simultaneously [19]. These measurements are combined with the film stoichiometry from ion scattering to calculate film densities. The estimated relative standard uncertainty has been found to be ±1% of the reported density [19].

The film morphology was examined by planar and cross-sectional scanning electron microscopy (SEM) using an accelerating voltage of 1.0 and 2.0 kV, respectively. In the case of the cross-sectional SEM, the converted film was broken in half using a diamond scribe. Atomic force microscopy (AFM) images were obtained in tapping mode. The scan sizes ranged from 1 to 30 μm^2 with a scan rate of 2.0 Hz. The film thickness and the refractive indices of the modified films were measured by ellipsometry.

3. Results and discussion

Using a wide variety of thin film analysis techniques, a rich phenomenology for the conversion of BCESSQ to an ormosil film was revealed. Thermal conversion yielded films with substantially different characteristics than films exposed to ultraviolet irradiation. In Section 3.1 we examine the effect of temperature on film thickness (Section 3.1.1), composition (Section 3.1.2), density (Section 3.1.3) and morphology (Section 3.1.4).

As an alternative to pyrolytic conversion, the BCESSQ films can be converted to ormosil films by exposure to ultraviolet light (UV) and ozone (Section 3.2). The UV produces ozone while also exciting the BCESSQ molecules. Initial studies are aimed at determining whether conversion is due to UV radiation, ozone or both (Section 3.2.1). Subsequent studies show the effect of exposure time on film thickness and refractive index (Section 3.2.2), and composition (Section 3.2.3) for BCESSQ films 224, 496, and 703 nm thick. Finally, film density measurements (Section 3.2.4) and morphology (Section 3.2.5) studies will be presented.

3.1. Temperature induced transformation studies

3.1.1. Film thickness

For pyrolytic conversion, the final film thickness is controlled by the as-cast film thickness, annealing time, and annealing temperature. After 4 h at 400°C, the final film thickness increases from about 100 to 450 nm as the mass fraction of BCESSQ concentration in diglyme increases from 5 to 50%, respectively. Whereas cracks covered about 10% of the total area of the 450 nm film,

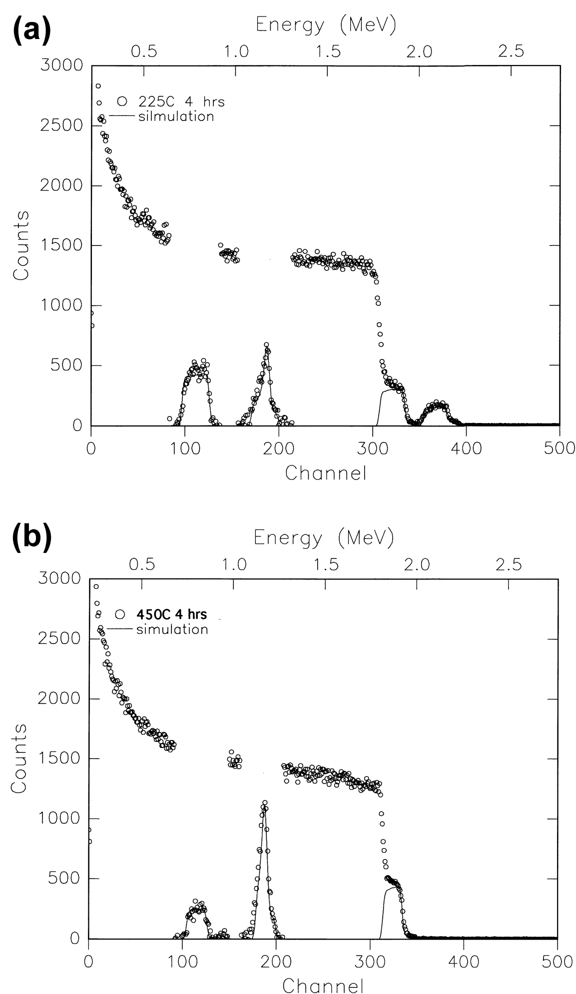

Fig. 6. Rutherford backscattering spectrometry spectrum for 3.4 MeV He^+ ions incident on a silicon substrate covered with a an ormosil film prepared from BCESSQ annealed for 4 h at (a) 225°C and (b) 450°C, respectively. The solid lines are simulations based on compositions in Table 1.

films ranging from 80 to 250 nm were smooth as observed in an SEM at 300 000 × magnification.

The film thickness after conversion normalized by the initial thickness, t_0, is shown in Fig. 4 for a BCESSQ film ($t_0 = 206.5$ nm) at 350°C. Within a few minutes, the normalized thickness rapidly decreases to about 68% (140.8 nm). After 20 min, this thickness decreases to 58%. For times longer than 20 min, the normalized thickness decreases more slowly, reaching a value of 52% (108.5 nm) after 5 h.

Fig. 5 shows how the normalized thickness decreases with increasing annealing temperature at a constant time of 2 h. The temperature range 350 to 450°C was chosen because TGA studies (cf. Section 2.2) show that densification occurs over this range. These results suggest that film densification increases smoothly with temperature, rather than abruptly at a well defined temperature.

3.1.2. Film composition

Whereas TGA-mass spectrometry is useful for bulk conversion studies, ion scattering is the technique of choice for determining thin film composition and areal density. Using the TGA studies as a guide, BCESSQ films about 200 nm thick were annealed at temperatures ranging from 225 to 450°C for 4 h. Figs. 6a and 6b show the 3.4 MeV $^4He^+$ RBS spectra for samples annealed at 225 and 400°C, respectively. At 225°C, the film contains chlorine, silicon (2.0 MeV), oxygen, and carbon (0.75 MeV). The two chlorine plateaus correspond to the two major isotopes. The dramatic increase in yield near 1.8 MeV represents the silicon signal from the substrate. The oxygen yield is superimposed on this silicon substrate background. The cross-section resonance at 3.045 MeV [20] produces the sharp peak in the oxygen signal. Using FRES to measure H, the atomic composition and areal density are $Si_{0.09}O_{0.16}C_{0.17}Cl_{0.05}H_{0.55}$ and 1000×10^{15} atoms/cm^2, respectively. In contrast to Fig. 6a, the chlorine signal in Fig. 6b is not observed at 450°C. Whereas the oxygen and carbon yields are similar in magnitude in Fig. 6a, the oxygen yield is significantly stronger than the carbon yield in Fig. 6b, suggesting a lower carbon content. Quantitatively, the stoichiometry and areal density are $Si_{0.18}O_{0.42}C_{0.10}H_{0.30}$ and 600×10^{15} atoms/cm^2 at 450°C.

Table 1 shows the stoichiometry for BCESSQ films annealed for 4 h in air. The as-cast composition is based on bulk solid state carbon and silicon NMR studies [12]. Note that this material has one silanol, Si—OH, for every three BCE groups, $Si—CH_2CH_2Cl$. After annealing at 225°C, the oxygen to silicon atom ratio is only 1.8, similar to that of the as-cast sample. Incomplete conversion is also suggested by the high carbon and chlorine atom fraction, 17 and 5%, respectively. It is important to note that the carbon:-chlorine ratio (≈3:1) is slightly in excess of 2:1, which is the BCE ratio. Because RBS is insensitive to bonding, the origin of the excess carbon is unknown. Note that the hydrogen concentration is also greater than expected. Possible sources of carbon and hydrogen include residual casting-solvent or trapped ethylene remaining from the conversion process. Note, however, that the carbon to hydrogen ratio is approximately 1:3 rather than the 1:2 ratio expected for ethylene. Because IR studies proved inconclusive, XPS studies will be needed to resolve this issue.

Upon increasing the temperature to 300°C, the chlorine concentration decreases to an atom fraction of 1% reflecting the high reactivity of chlorine. However, the carbon concentration does not change appreciably. If the BCE reaction followed previous TGA-MS studies, the evolution of ethylene (loss of carbon) would be expected. A comparison of the silicon and carbon atom fractions, 14 and 17%, respectively, provides important insight into the conversion process at elevated temperatures. Namely, these compositions suggest that approximately half of the silicon atoms are bonded to vinyl groups, $Si—CH{=}CH_2$. Thus, the higher temperature gives complete reaction of the BCE groups, but little change in the carbon concentration, relative to the 225°C conversion, because of the possible formation of

Table 2
Thin film densities after thermal conversion in air

Temperature (°C)	Density (g/cm^2)	Thermal oxide (%)
As-cast	1.45	64
225	1.57	70
350	1.53	68
450	1.88	84

vinyl groups. These observations are consistent with ^{13}C NMR studies on BCESSQ annealed at 300°C [12]. In these studies, the BCE chlorine reacted to form HCl leaving a vinyl group bound to Si. This second pathway for BCE reaction is the likely source of residual carbon.

At 400°C, the oxygen to silicon ratio increases to 2.1:1. At this temperature, chlorine in the film is no longer observed (<0.2% atom fraction), suggesting that all BCE groups have reacted. Some BCE groups react cleanly and evolve ethylene, whereas others form vinyl groups and evolve HCl. Both the hydrogen and carbon concentrations are less than the low temperature studies. As the temperature increases from 300 to 400°C, the silicon to carbon ratio increases from ≈0.8 to ≈1.2, respectively. This result is consistent with the oxidation of vinyl groups to produce $Si—CH_3$, which lowers the C concentration. In fact, NMR studies show that vinyl groups undergo further reaction with oxygen to yield a methyl group with the formation of carbon dioxide at 370°C [12]. Note that the carbon to hydrogen ratio is 1:2.7, close to the value expected for a methyl group. Annealing at 450°C reduces the carbon content to even lower values while maintaining a C:H ratio of 1:3. This decrease in carbon is attributed to further oxidation of residual methyl groups. Because the Si—C bond is relatively stable, incomplete conversion results because cross-links of Si—O—Si are prevented from forming. Although incomplete conversion should lower the O:Si ratio, Table 1 shows that the ratio is 2.3 suggesting an oxygen excess at 450°C. This excess may reflect trapped small molecules including CO_2, CO and H_2O.

Ion scattering studies clearly show that appreciable concentrations of carbon and hydrogen remain in films cured at temperatures ranging from 225 to 450°C. NMR studies [12] show that these organic groups are bound to silicon atoms. Thus, films prepared from BCESSQ can be classified as ormosils. As mentioned previously, the dielectric constant of ormosils can be controlled by tailoring the carbon concentration [9,31].

For comparison, ion analysis experiments were performed on commercial dielectric materials, namely Accuspin® 720 and Accuglass® 311. After annealing (cf. Section 2.1), RBS and FRES were used to determine the compositions which were $Si_{0.07}O_{0.09}C_{0.17}H_{0.66}$ and $Si_{0.18}O_{0.33}C_{0.12}H_{0.37}$, respectively. For Accuspin®, the low O:Si ratio, 1.3:1, and high carbon content, 17% atom fraction, results from the incomplete reaction of silicon atoms bonded with the relatively stable methyl groups. Note that the hydrogen to carbon ratio is about 4 to 1, slightly in excess of the 3 to 1 ratio expected for a methyl group. For Accuglass®, the oxygen to silicon ratio is 1.9:1, suggesting nearly complete conversion. However, judging completion by the O:Si ratio is misleading because ion beam analysis clearly shows that Accuglass® still retains significant carbon (12% atom fraction) and hydrogen (37% atom fraction) content. For both Accuspin® 720 and Accuglass® 311, the C and H contents are greater than those found in BCESSQ films converted at 450°C. One important outcome of this study on dielectric materials is the need to quantify the hydrogen content which can be an atom fraction as great as 70%.

3.1.3. Film density

Energy dispersive XR is used to measure the mass densities of the thermally converted BCESSQ films presented in Section 3.1.2 and Table 1. Because XR measures the electron density, mass density can be determined using the compositions in Table 1. The thin film mass densities are presented in Table 2. The mass density of the as-cast BCESSQ film is 1.45 g/cm^3. For comparison, this value is much greater than that of a cross-linked poly(dimethylsiloxane), rubber, 0.98 g/cm^3 [21]. Annealing at 225 and 350°C produces films with densities of 1.57 g/cm^3 and 1.53 g/cm^3, values only slightly higher than the as-cast film. These densities are within the experimental uncertainty of each other. The relatively low densification is consistent with the high carbon and hydrogen concentrations remaining in the film. As a reference, silicon dioxide films grown in oxygen, wet oxygen, or steam at temperatures ranging from 900 to 1200°C have densities of about 2.25 g/cm^3 [5,22]. Thus for the films annealed at 225 and 350°C, the densities are only about 70% of thermally grown oxides. However, at 450°C the density increases to 1.88 g/cm^3 or 84% of thermal oxide. This densification may be attributed to the evolution of hydrocarbons and the subsequent filling of pores by oxide reflow. It is interesting to note that pyrolytic oxides densify at much higher temperatures (>800°C) [22].

3.1.4. Microscopy of thermally converted films

The morphology and surface roughness were studied using SEM and AFM, respectively. For a BCESSQ film annealed at 400°C for 2 h in air, top-view SEM images show a smooth featureless surface at magnifications of 1000, 30 000 and 50 000. SEM from a film cross-section shows that the film/silicon interface exhibits no voids or cracks, suggesting good adhesion. To directly test adhesion, a piece of scotch tape was adhered to the film and quickly removed. In all cases, the ormosil films remained firmly attached to the silicon substrates.

AFM studies show that the ormosil films are quite smooth. For two sets of samples, AFM images were obtained from films ranging from about 200 to 800 nm. One set was annealed at 350°C and the other at 450°C for

Table 3
Normalised thickness and surface roughness after thermal conversion for 2 h in air

Temperature (°C)	Initial thickness (nm)	Final thickness (nm)	Shrinkage (%)	Roughness (nm)
350	204.2	115.1	56	0.32
350	583.3	347.2	59	0.84
350	744.5	580.6	76	0.40
450	207.3	103.3	50	0.51
450	614.7	337.6	55	1.47
450	792.8	559.9	71	0.39

2 h. Table 3 shows the film thickness before and after annealing, film shrinkage, and roughness. The shrinkage of the thinnest films at both temperatures are consistent with the bulk mass loss of 52.5%. However, the thicker films do not decrease in thickness as much as the thinner films suggesting a depth dependent conversion mechanism. For HSSQ annealed in a furnace, incomplete conversion has been attributed to initial conversion of the outermost film causing a 'skinover' which limits the diffusivity of oxygen needed to convert the film further beneath the surface [23]. Over a lateral area of 1×1 μm, the root-mean-square roughness measurements range from 0.3 to 1.5 nm. This roughness appears independent of the final film thickness.

3.2. Ultraviolet irradiation studies at room temperature

3.2.1. Role of ozone

To understand the role of UV and ozone in converting BCESSQ to ormosil, two 200 nm films are prepared from a diglyme solution with 15% mass fraction BCESSQ. One film is exposed to UV under normal atmospheric conditions and its thickness measured periodically by ellipsometry. The other film is exposed to UV while the sample compartment is continuously purged with nitrogen. The normalized film thickness as a function of UV exposure time is shown in Fig. 7. In air, the film thickness decreases rapidly, to about 55%, within the first hour. After 2 h, the normalized thickness approaches a constant value of about 49%, which is comparable to that achieved by pyrolytic conversion at high temperatures (cf. Figs. 4 and 5). In particular, UV-ozone conversion provides an attractive route for preparing interlayer dielectrics because thermal stress should be reduced relative to pyrolytic conversion. For the BCESSQ film exposed to UV in a nitrogen purge, the normalized film thickness decreases at a similar rate as the sample exposed in air.(Because the sample compartment was not entirely sealed, some ozone could have been produced during the UV exposure. Nonetheless, the ozone concentration would be reduced and, therefore, BCESSQ conversion would slow down.) This result indicates that ultraviolet exposure, not the reaction of ozone with BCESSQ, is mainly responsible for the conversion of BCESSQ. Using laser irradiation to induce BCESSQ transformation, recent studies show that the 193 nm UV radiation is likely responsible for the removal of hydrocarbon [28].

Mirley and Koberstein [24] have prepared thin silica films by exposing a multilayer Langmuir–Blodgett film of carboxylic acid-terminated PDMS to a UV-ozone cleaner with a mercury-quartz lamp. After 30 min, the near-surface converts to a 14.1 nm thick silica layer, whereas the bottom 9.1 nm layer remains PDMS. The authors interpret these results as indicating a diffusion-controlled reaction of PDMS, which is limited by ozone diffusion through outer silica layer. In contrast, the BCESSQ film conversion is driven by UV irradiation, not ozone reaction. To further

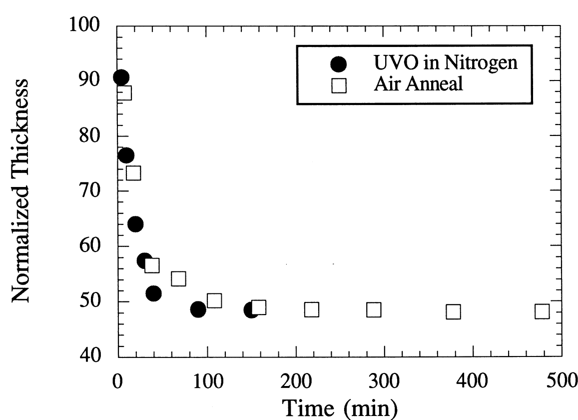

Fig. 7. Normalized film thickness as a function of ultraviolet exposure time in air (□) and in nitrogen (●).

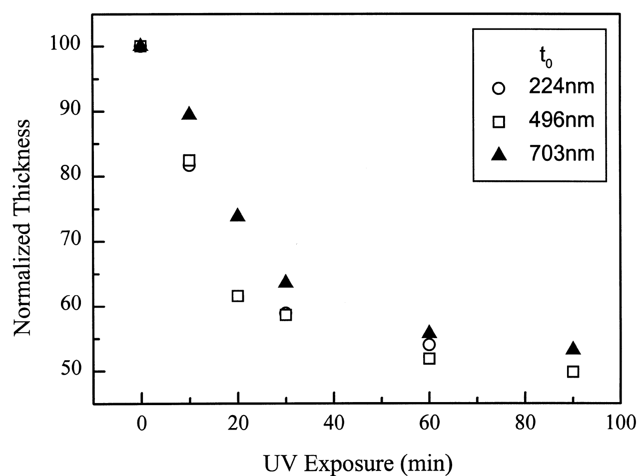

Fig. 8. Normalized film thickness as a function of UV-ozone exposure. Before conversion, the films have a thickness of 224, 496, and 703 nm.

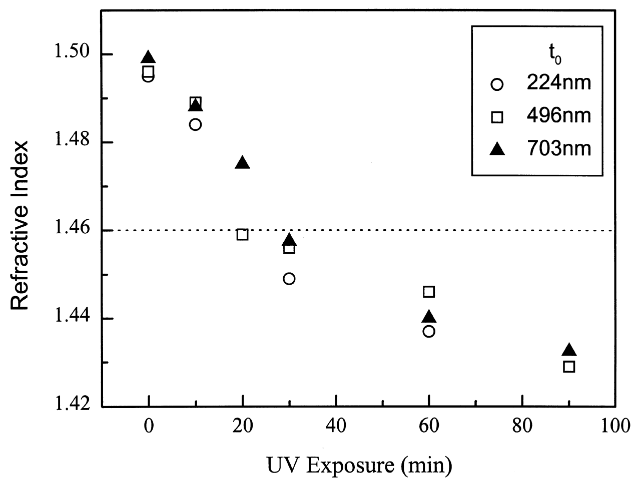

Fig. 9. Refractive index of ormosil films as a function of UV-ozone exposure time. The films are the same as in Fig. 8. The dotted line marks the refractive index for fused silica.

explore if conversion varied with depth, films of various thicknesses were exposed to UV ozone.

3.2.2. Film thickness and refractive index

The BCESSQ film thickness and refractive index as a function of UV-exposure is investigated for t_0 of 224, 496, and 703 nm. Fig. 8 shows how the normalized thickness decreases with exposure time. During the first 30 min, the film thickness decreases rapidly to about 60%. After 30 min, the film thickness decreases much more slowly and approaches ca. 50% asymptotically with time. These observations demonstrate that UV radiation induces the transformation of BCESSQ mainly during the first 30 min. The films 224 and 496 nm thick show a nearly identical change in thickness with time. The thickest film, however, shows a slightly slower decrease in thickness suggesting that the layer adjacent to the silicon substrate may be unmodified BCESSQ. Although ion scattering experiments suggest a uniform depth profile, techniques with a higher depth reso-

Fig. 10. Ormosil film composition as a function of UV-ozone exposure time for BCESSQ films having a thickness of 224, 496, and 703 nm. The (a) O:Si, (b) C:Si, (c) Cl:Si and (d) H:Si ratios are given. The dotted lines denote the elemental ratios for SiO_2. The sensitivity and uncertainties are discussed in Section 2.4.

Table 4
Thin film densities after UV-ozone exposure

Exposure time (min)	Density (g/cm^2)	Thermal oxide (%)
As-cast	1.44	64
6	1.50	67
12	1.57	70
24	1.71	76

lution (e.g. Auger electron spectroscopy) are needed to support this observation.

One surprising result was that UV ozone conversion reduces film thickness as effectively as thermal treatment (cf. Figs. 8 and 3, respectively). In contrast, the photoinduced transformation of polysiloxane films requires simultaneous heating in excess of 350°C to induce the final condensation reaction [25]. Such temperatures allow for out-diffusion of trapped species and void sealing. Subsequent studies by Joubert et al. [29] suggest that laser induced heating is required to convert polysiloxane films to amorphous SiO_2. Using a very low pulse energy compared to [29], we have found that laser irradiated BCESSQ films fully convert as demonstrated by the films final thickness and lack of carbon [28]. However, in contrast to [28] and [29], the temperature rise in our study was held to less than 100°C which suggests that optically induced bond breaking does play a role in the conversion process.

The refractive indices are shown as a function of exposure time in Fig. 9. For all three films, the refractive indices decrease monotonically from ca. 1.498 to 1.430, indicating a significant conversion of the films. This behavior mirrors the film thickness decrease in Fig. 8. After 20 min, the refractive index is ca. 1.46. For comparison, thermal oxide films (300–800 nm) and fused silica have indices of 1.4618 and 1.4601 at 546 nm [26]. After 20 min, the refractive index becomes less than 1.46 possibly because of film stoichiometry and/or

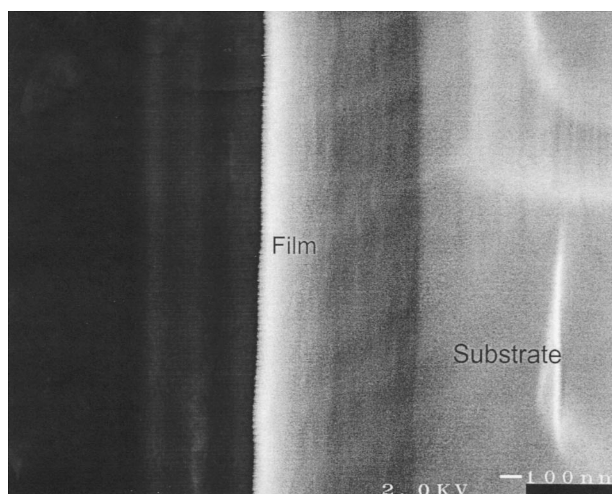

Fig. 11. Cross-sectional SEM image for a BCESSQ film exposed to UV irradiation for 120 min. The sample is tilted to facilitate observation of film quality.

pores. Both contributions will be explored in Section 3.2.3 and Section 3.2.4.

3.2.3. Film composition

The film composition for the UV-ozone exposed films is determined by ion scattering. Figs. 10a,b,c,d show the oxygen:silicon, carbon:silicon, chlorine:silicon and hydrogen:silicon ratios, respectively, for the same three films presented in Section 3.2.2. Within experimental error, the composition ratios are independent of thickness suggesting that conversion is uniform through the film thickness. The O:Si ratio increases rapidly from about 1.4 to 2.0 as exposure time increases from 0 to 10 min. This ratio continues to increase with exposure time, reaching a value of 2.2 after 30 min. Recall that BCESSQ films annealed at 400 and 450°C also contained excess oxygen relative to SiO_2 (cf. Table 1). As shown in Fig. 10b, the C:Si ratio decreases from two carbons per silicon towards zero as exposure time increases from 0 to 90 min. Whereas the O:Si ratio is relatively constant after 20–30 min exposure time, the carbon concentration is relatively high after this time and continues to decrease with further exposure. Thus the carbon evolves from the sample relatively slowly. The H:Si ratio also decreases relatively slowly with exposure time. Even after 90 min, the atom fractions of hydrogen and carbon are about 0.20 and 0.02, respectively. The Cl:Si ratio decreases much faster than the C:Si and H:Si ratios. After 30 min, the atom fraction of chlorine is less than 1.0%. Note that the Cl:Si ratio decreases at a similar rate as the O:Si increases (cf. Figs. 10a and 10c).

For films exposed to UV-ozone radiation, the BCESSQ reaction mainly occurs over the first 30 min. The rapid decrease in chlorine content reflects the high reactivity of this species relative to the ethylene linkage on the BCE group. The reason for the slower evolution of C and H could be due to the slow diffusion of hydrocarbons and/or CO_2 out of the glassy film. On the other hand, in the UV-ozone modified films the carbon content is 10× less than the concentration in films annealed at 450°C. Although relatively chlorine free and containing a low carbon concentration, films exposed for 90 min still retain a high hydrogen concentration, ca. 20 % atom fraction. Possible sources of H include H_2O produced during conversion or adsorbed from the atmosphere. Water adsorption is also consistent with the excess oxygen content (i.e. O:Si ratio >2) and the low refractive index (cf. Fig. 9).

3.2.4. Film density

The density of films converted by UV-ozone exposure was determined by energy-dispersive X-ray reflectivity in conjunction with the composition from ion scattering. Table 4 shows that the film density increases monotonically with exposure time. After 24 min, the density is 1.71 g/cm^3 which is 76% of thermal silicon oxide. Thus, UV-ozone treatment produces films only slightly less dense than the best thermal treated films (1.88 g/cm^3). Fig. 10b, d show that the C and H

concentrations, respectively, can be reduced by longer exposures (i.e. 60 min). Thus, densities greater than 1.71 g/cm^3 are possible. For UV-ozone exposed films, densification likely proceeds by radiation-induced detachment of BCE, the release of gaseous molecules, and finally void sealing [27]. Initially, pores can be filled because of the low viscosity of BCESSQ, which is only lightly cross-linked. As the BCESSQ reaction proceeds, the film hardens and the removal of gaseous species becomes more difficult.

3.2.5. Cross-section microscopy

Scanning electron microscopy was used to characterize film quality. Fig. 11 shows a cross-section of a BCESSQ film after a 120 min UV exposure. The sample is tilted with respect to the incident beam. The ormosil film is located in the center of the image. Because it is an insulator, the film charges as denoted by the white strip on the film surface. The silicon substrate is on the right (light gray). The uniform film thickness and sharp interface with silicon demonstrate that the film quality is excellent. The former observation is consistent with the small surface roughness found by AFM (cf. Table 3). No pores are observed at this magnification.

4. Conclusions

The pyrolytic and photolytic conversion of a new polymer precursor, namely β-chloroethyl-silsesquioxane (BCESSQ), to an ormosil film is studied. Ormosil films have been prepared at temperatures as low as 225°C. With increasing temperatures, a systematic decrease in carbon, hydrogen and chlorine concentration is observed. Compared to Accuglass® 311, ormosil films prepared by heating BCESSQ at 450°C have lower carbon and hydrogen concentrations. At 450°C, the film density is 1.88 g/cm^3, or 84% of a thermal silicon oxide. For a 100 nm film, AFM and SEM studies show that the ormosil surface is smooth, the bulk is void free at 50 000 ×, and the ormosil/substrate interface is continuous. Upon exposure to ultraviolet-ozone radiation, BCESSQ films ranging from ca. 200 to 700 nm are found to convert to ormosil films within ca. 30 min. Surprisingly, the chlorine concentration is found to decrease more quickly than the hydrogen and carbon concentrations, suggesting that the ormosil film evolves HCl initially leaving a vinyl group of $Si{-}CH{=}CH_2$. This reaction pathway differs from the thermal case. Although having lower carbon atom fractions (2 vs. 10%) and hydrogen (20 vs. 30 %) than the pyrolytic films, the UV-ozone films had a lower density (e.g. 1.71 vs. 1.88 g/cm^3). This result suggests that the reaction and/or by-product release can readily occur in the UV-ozone case, however, higher densities can only be achieved with some thermal processing.

Acknowledgements

This work was supported primarily by the MRSEC Program of the National Science Foundation under Award DMR96-32598. We acknowledge use of the MRSEC shared experimental central facilities of the LRSM at the University of Pennsylvania for ion scattering, AFM, and SEM studies. RJC acknowledges partial support from the Division of Materials Research at NSF under Award DMR95-26357. We acknowledge assistance from Bruce Rothman, Dan Polis, Rollin Lakis, Jaya Sharma, Hai-Lung Dai, and Raymond Hsaio.

References

[1] G.K. Rao, Multilevel Interconnect Technology, McGraw-Hill, New York, 1993.
[2] W.W. Lee, P.S. Ho, MRS Bulletin 22 (10) (1997) 19.
[3] Handbook of Multilevel Metallization for Integrated Circuits, in: S.R. Wilson, C.J. Tracy, J.L. Freeman Jr (Eds.), Materials, Technology, and Applications, Noyes Publications, Park Ridge, NJ, 1993.
[4] T.-M. Lu, J.A. Moore, MRS Bulletin 22 (10) (1997) 28.
[5] W.A. Pliskin, J. Vac. Sci. Technol. 14 (1977) 1064.
[6] J.-H. Kim, S.-H. Seo, S.-M. Yun, H.-Y. Chang, K.-M. Lee, C.-K. Choi, Appl. Phys. Lett. 68 (1996) 1507.
[7] D. Seyferth, Adv. Chem. Ser. 224 (1990) 565.
[8] R.H. Baney, M. Itoh, A. Sakakibara, T. Suzuki, Chem. Rev. 95 (1995) 1409.
[9] N.P. Hacker, MRS Bulletin 22 (10) (1997) 33.
[10] H.K. Schmidt, in: M. Zeldon, K.J. Wynne, H.R. Allcock (Eds.), ACS Symposium Series 360, American Chemical Society, Washington DC, 1988.
[11] B. Arkles, D.H. Berry, L.H. Figge, R.J. Composto, T. Chiou, H. Colazzo, W.E. Wallace, J. Sol-Gel Sci. Tech. 8 (1997) 465.
[12] Lisa Kiernan Figge, Ph.D. Dissertation, University of Pennsylvania, 1996.
[13] L.R. Doolittle, Nucl. Instr. Methods B9 (1985) 344.
[14] L.R. Doolittle, Nucl. Instr. Methods B15 (1986) 227.
[15] J.A. Leavitt, L.C. McIntyre Jr., P. Stoss, J.G. Oder, M.D. Ashbaugh, B. Dezfouly-Arjomandy, Z.M. Yang, Z. Lin, Nucl. Instr. Methods B40/41 (1989) 776.
[16] J. Genzer, J.B. Rothman, R.J. Composto, Nucl. Instr. Methods B86 (1994) 345.
[17] J. Li, F. Moghadam, L.J. Matienzo, T.L. Alford, J.W. Mayer, Solid State Technol. 38 (5) (1995) 61.
[18] W.-K. Chu, J.W. Mayer, M.-A. Nicolet, Backscattering Spectrometry, Academic Press, Orlando, 1978.
[19] W.E. Wallace, W.L. Wu, Appl. Phys. Lett. 67 (1995) 1203.
[20] J.A. Leavitt, L.C. McIntyre Jr., M.D. Ashbaugh, J.G. Oder, Z. Lin, B. Dezfouly-Arjomandy, Nucl. Instr. Methods B44 (1990) 260.
[21] F. Rodriguez, Principles of Polymer Systems, 2nd Ed., McGraw-Hill, New York, 1982.
[22] W.A. Pliskin, H.S. Lehman, J. Electrochem. Soc. 112 (1965) 1013.
[23] T.E. Gentle, Proc. SPIE 1595 (1991) 146.
[24] C.L. Mirley, J.T. Koberstein, Langmuir 11 (1995) 1049.
[25] A. Klumpp, H. Sigmund, Appl. Surf. Sci. 43 (1989) 301.
[26] W.A. Pliskin, H.S. Lehman, J. Electrochem. Soc. 112 (1965) 1013.
[27] R.E. Schenker, W.G. Oldham, J. Appl. Phys. 82 (1997) 1065.
[28] J. Sharma, D.H. Berry, R.J. Composto, H.L. Dai, J. Mater. Res., (in press).
[29] O. Joubert, G. Hollinger, C. Fiori, R.A.B. Devine, P. Paniez, R. Pantel, J. Appl. Phys. 69 (1991) 6647.
[30] M. Nastasi, J.R. Tesmer (Eds.), Handbook of Modern Ion Beam Materials Analysis Materials Research Society, Pittsburgh, PA, 1995.
[31] N.P. Hacker, G. Davies, L. Figge, T. Krajewski, S. Lefferts, J. Nedbal, R. Spear, Mater. Res. Soc. Symp. Proc. 476 (1997) 25.